

Polarization Insensitive and Broadband Terahertz Absorber Using Graphene Disks

Kamalodin Arik¹ · Sajjad AbdollahRamezani¹ · Amin Khavasi¹

Received: 9 December 2015 / Accepted: 31 May 2016 / Published online: 14 June 2016
© Springer Science+Business Media New York 2016

Abstract We demonstrate design and characterization of a polarization-independent ultra-broadband absorber of light consisting of periodic array of graphene disks on top of a lossless quarter-wavelength dielectric spacer placed on a metallic reflector. The absorber is duly designed based on impedance matching concept by proposing a fully analytical circuit model resulting in a normalized bandwidth of 100 % in the terahertz regime.

Keywords Broadband absorber · Graphene disks · Circuit model

Introduction

The absorption of incident radiation can be efficiently achieved by electromagnetic wave absorbers over a broad wavelength range. The broadband property of absorbers is of great importance in many devices such as solar energy-harvesting devices [1], bolometers [1], dummy loads [2], thin-film thermal emitters [3], and plasmonic scatters [4]. Various approaches have been proposed for achieving broad absorption band. Many of them are based on embracing multiple resonators with relatively small differences in size within the same unit cell. Accordingly, several distinct narrow band resonant absorbers can be mixed to develop broadband absorption [5]. Ye et al. [6] and Grant et al. [7] presented broadband absorbers made of

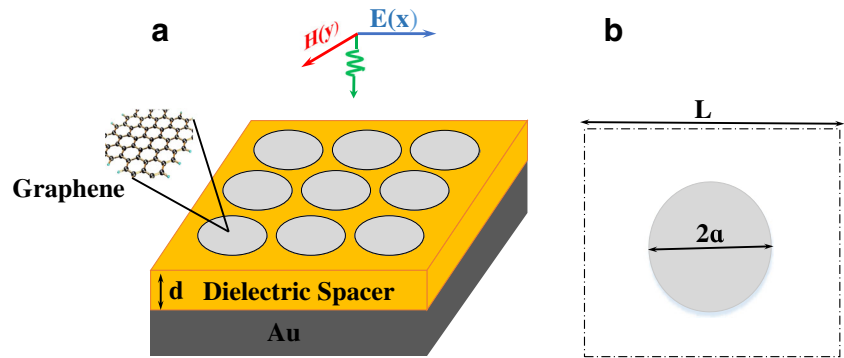
vertical and horizontal integration of such distinctly sized resonators, respectively. However, these methods impose a complicated fabrication process [8] and a limited normalized absorption bandwidth (normalized to the central frequency) [5]. More recently, a method for achieving broadband absorption using impedance matching concept has been proposed, and normalized absorption bandwidth of 100 % has been achieved using periodic array of graphene ribbons [9]. Nonetheless, since the proposed structure is polarization-dependent, only absorbs TM-polarized waves (magnetic field along the ribbons).

In this work, we investigate a well-designed polarization-independent ultra-broadband terahertz (THz) absorber. The absorber consists of a periodic array of graphene disks on a lossless thin dielectric layer and a reflecting backplate placed at the bottom. The proposed absorbing structure is designed based on impedance matching concept. To this end, we use the analytical circuit model reported in [10] for periodic array of graphene disks. We then assign an equivalent circuit to the absorber and choose the input admittance of the circuit close to that of free space at the central frequency to obtain high absorption. Furthermore, an additional condition on the derivative of input admittance is applied for widening the absorption band. Therefore, we will come to see a normalized bandwidth of 100 %. This method of design is then verified through full-wave simulations. It should be noticed that the proposed absorber is polarization insensitive for normal incident EM waves owing to its symmetric structure. Moreover, the broadband and the near-perfect absorption efficiency is only slightly affected even at high angles of incidence for both TE and TM polarizations. In addition, we show that the proposed absorber exhibits a wide-angle absorption and negligible sensitivity with respect to fabrication uncertainties. The rest of the paper is organized as follows. In

✉ Amin Khavasi
khavasi@sharif.edu

¹ Department of Electrical Engineering, Sharif University of Technology, P.O. Box 11555-4363, Tehran, Iran

Fig. 1 **a** Schematic representation of the proposed absorber composed of a middle layer of dielectric spacer sandwiched between a top layer of graphene disks and a bottom layer of Au ground plate. The structure is illuminated at normal incidence **(b)**. A unit cell of periodic array of graphene disk



“Circuit Model of the Proposed Absorber”, the structure of the absorber is presented and an equivalent circuit for this structure is proposed. “Design Procedure” outlines the design procedure and closed expressions are derived for the appropriate parameters required for achieving broadband absorption. The limitations of the proposed design are presented in “Limitations.” Finally, conclusions are drawn in “Conclusion”.

Circuit Model of the Proposed Absorber

The geometry of the proposed absorber is schematically shown in Fig. 1 in which the top layer of periodic array of graphene disks with radius a and the bottom layer of optically opaque Au ground plate with finite conductivity of $\sigma = 4 \times 10^7 \text{ S/m}$ are separated by a dielectric spacer with refractive index of $n_s = 1.5$ and thickness of d . The disks are located on the corners of a square lattice whose lattice constant (period of the array) is denoted by L . Due to the structure’s symmetry, polarization-independent absorption spectra at normal incidence is expected. Hence, we consider only one polarization: E field polarized along the x -axis. The equivalent circuit for the proposed absorber is illustrated in Fig. 2 in which the Au backplate which is suppressing the transmittance is represented by the admittance $Y_{Au} \rightarrow \infty$. Simulation results show that this is a good approximation at terahertz frequencies. The homogeneous mediums namely the free space and the dielectric spacer

are modeled as transmission lines with propagation constant $\beta = 2\pi n/\lambda$ and admittance $Y = n/\eta_0$ where n and η_0 are refractive index of corresponding region and free-space intrinsic impedance, respectively, and λ represents the free-space wavelength. The disk array is modeled by a shunt admittance Y_G which represents an infinite number of parallel R-L-C circuits, each corresponding to one mode of graphene disk [10, 12, 13]. Designing the proposed device near the first mode, we just retain the corresponding R-L-C branch as the circuit model of the graphene disk arrays. Our simulations show that neglecting the effect of higher order modes of the disk arrays maintain an insignificant effect on the accuracy of the model, so, we have

$$Y_G \cong \frac{\pi^2}{L^2} \left(\sigma_s^{-1} + \frac{q_{11}}{j\omega\epsilon_{eff}} \right)^{-1} \frac{S_1^2}{K_1} \quad (1)$$

where q_{11} is the first eigenvalue of the equation governing the current on the disks (values of q_{11} for different $2a/L$ have been given in table (2) of [10]), $S_1 = 0.6087a$, $K_1 = 1.2937$, and $\epsilon_{teff} = \epsilon_0(1 + n_s^2)/2$ is the average permittivity of the mediums surrounding the disks. At sufficiently low frequencies, surface conductivity of graphene would be presented by the Drude model [11]. Therefore, after some straightforward manipulations, Eq. 1 can be rewritten as follows:

$$Y_G = \frac{1}{R_1 + L_1 j\omega + \frac{1}{C_1 j\omega}} \quad (2)$$

$$R_1 = \frac{\hbar^2}{e^2 E_f \tau} \frac{K_1 L^2}{\pi S_1^2} \quad (3)$$

$$L_1 = \frac{\hbar^2}{e^2 E_f} \frac{K_1 L^2}{\pi S_1^2} \quad (4)$$

$$C_1 = \frac{\epsilon_{eff} \pi^2 S_1^2}{q_{11} K_1 L^2} \quad (5)$$

where E_f and τ are the Fermi level and the relaxation time. We could thus assign the circuit shown in Fig. 2 to the proposed device. The input admittance of the circuit is then computed as,

$$Y_{in} = Y_{Au}^{tr} + Y_G \quad (6)$$

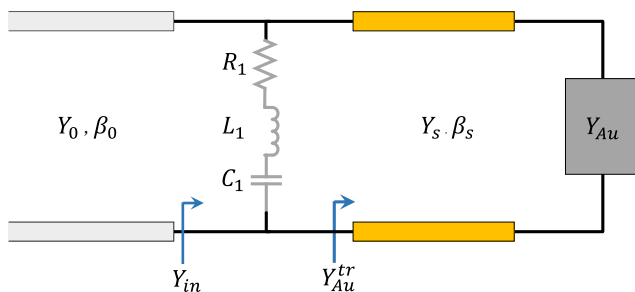


Fig. 2 The equivalent circuit of the proposed absorber

$$Y_{Au}^{tr} = Y_s \frac{Y_{Au} + jY_s \tan \beta_s d}{Y_s + jY_{Au} \tan \beta_s d} \tag{7}$$

where β_s and Y_s are the propagation constant and the admittance of the transmission line corresponding to the dielectric spacer, respectively.

Design Procedure

In this section, we design the proposed absorber based on the circuit obtained in the last section. Impedance matching concept will be used to extract closed expressions for the device parameters. We know that the transmission channel is closed by the Au backplate. So, in order to maximize the absorption of the device, a minimum reflection is needed. To this end, the circuit should be impedance matched to that of free space. Hence, at the central frequency, f_0 , the conditions $\text{Re}(Y_{in}) = Y_0 = 1/\eta_0$ and $\text{Im}(Y_{in}) = 0$ should be satisfied. By setting $\beta_s d = \pi/2$ at f_0 , from Eq. 7 $Y_{Au}^{tr} = 0$, so, according to Eq. 6 the admittance of the graphene array is observed as the input admittance of the structure. Therefore, the two above conditions are simplified as follows:

$$R_1 = \eta_0 \tag{8}$$

$$L_1 C_1 = \frac{1}{(2\pi f_0)^2} \tag{9}$$

By applying the Eqs. 8 and 9, perfect absorption is realized at the given central frequency. However, they would not lead to broadband absorption. Achieving a broadband absorption (not necessarily perfect), we relax the Eq. 8 and apply an additional condition on the derivative of the imaginary part of input admittance as follows:

$$R_1^{-1} = \frac{\alpha}{\eta_0} \tag{10}$$

$$\frac{d}{df} \text{Im}(Y_{in}) = 0 \tag{11}$$

in which α is larger than unity, but in order to fulfill reflection

$$\left(\frac{\frac{\eta_0}{\alpha} - \eta_0}{\frac{\eta_0}{\alpha} + \eta_0} \right)^2 < 0.1 \tag{12}$$

which results in $\alpha < 1.925$. We set $\alpha = 1.75$ throughout this work. It should be noted that a small imaginary part of the input admittance is achieved in wide range of frequencies around the central frequency as a result of applying the Eq. 11. The real part of the structure’s admittance, on the other hand, is close to that of the free space leading to negligible amount of reflection in this frequency range.

Now let us extract the device parameters using the invoked conditions. After some mathematical manipulations, Eq. 11 reduces to [9]:

$$\tau = \frac{n_s}{8\alpha f_0} \tag{13}$$

The parameters f_0 and n_s are assumed to be given, so the desired τ is obtained by tuning the Fermi level according to:

$$E_f = \frac{\tau e v_f^2}{\mu} \tag{14}$$

where μ is the electron mobility and $v_f = 10^6$ m/s is the Fermi velocity.

Furthermore, from $\beta_s d = \pi/2$ at f_0 , we obtain the following:

$$d = \frac{c}{4n_s f_0} \tag{15}$$

On the other hand, using Eq. 3, the ratio of the diameter of graphene disks and the square lattice constant is computed as follows:

$$\frac{2a}{L} = \sqrt{\frac{K_1 \hbar^2}{0.093\pi E_f \tau R_1 e^2}} \tag{16}$$

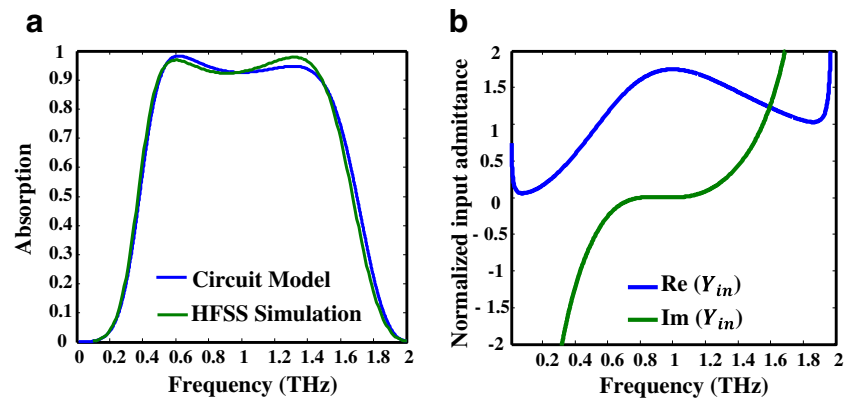
Finally, the radius of disks can be easily determined by substituting Eqs. 4 and 5 in Eq. 9:

$$a = \frac{r_1 E_f e^2}{\pi \epsilon_{eff} \hbar^2 \omega_0^2} \tag{17}$$

where $r_1 = a q_{11}$ and $\omega_0 = 2\pi f_0$.

To verify the proposed procedure, an ultra-broadband absorber based on the obtained formulas for a central frequency of $f_0 = 1$ THz is designed. The electron mobility is assumed to be $\mu = 0.2$ m²/Vs. Hence, the relaxation time and Fermi level are calculated as $\tau = 1.07 \times 10^{-13}$ s and $E_f = 0.595$ eV from Eqs. 12 and 13. The dielectric spacer thickness, on the other hand, is given by Eq. 16 as $d = 50$ μm. Finally, from Eqs. 15 and 16, we obtain $a = 49.62$ μm and $L = 106.14$ μm. Figure 3 shows the absorption spectrum for the designed absorber using the circuit model and full-wave simulation (HFSS). The HFSS simulation is carried out on a single period of the structure. In order to simulate infinite media in the transverse direction, a master-slave (M/S) relationship is defined between each of the periodic boundary condition (PBC) pairs. The floquet ports on the other boundaries simulated a plane wave propagating through the medium. In the full-wave analysis setup, graphene is modeled by an ultrathin layer of thickness $\Delta = 1$ nm whose relative permittivity is $\epsilon_{gr} = 1 + \sigma_s / j\omega \epsilon_0 \Delta$, where σ_s is the surface conductivity of graphene [12]. An excellent agreement is observed between the two results. Moreover, normalized bandwidth of 100 % has been attained. We have also plotted the real and imaginary part

Fig. 3 **a** Simulated absorption spectrum of the designed device whose parameters are $d = 50 \mu\text{m}$, $a = 49.62 \mu\text{m}$, and $L = 106.14 \mu\text{m}$ for normal incidence using the proposed circuit model and the full-wave simulation (HFSS). **b** Real and imaginary part of the normalized input admittance of the designed structure which indicate an approximate wide-band impedance matching condition at the central frequency of $f_0 = 1 \text{ THz}$



of the normalized input admittance Y_{in}/Y_0 using the proposed circuit model in Fig. 2. This figure reveals a near-zero imaginary part and a near-unity real part for the normalized input admittance around the central frequency indicating a wideband impedance matching and broadband absorption. Furthermore, such a symmetrical geometry which exhibits the same responses for both polarizations at normal incidence can maintain a strong and broadband absorption even at high angles of incidence for both TE and TM polarizations. Figure 4 plots the absorption spectra of light as function of frequency and incident angle for both polarizations. A broadband absorption of around 80 % is still achieved at incident angle of 70° for TM polarization and 60° for TE polarization. Hence, the proposed structure has a good performance over a broad range of incident angles for both TM and TE polarizations. Moreover, at small incident angles, a substantial overlap is observed between the absorption spectra for both polarizations. The proposed device is thus eligible to be polarization-independent absorber, at least for small incident angles.

The influence of some geometrical parameters on the absorption performance is also investigated. As it is obvious from Fig. 5, a fractional variation of $\pm 5\%$ in the disks

radius and the arrays period yields slight deviation in the absorption spectrum.

We note that the major effect responsible for the absorbance in the proposed structure is the excitation of localized plasmons on graphene disks. Figure 6 demonstrates that the efficiency of the absorber is significantly reduced in the absence of graphene. High absorption is thus caused by a series R-L-C resonance due to the coupling of incident light to localized plasmons supported by graphene disks.

Limitations

Although no limitation was imposed on the central frequency in the previous sections, it can not be chosen arbitrarily. The first limitation originates from the fact that the ratio $2a/L$ must be smaller than unity. Considering the conservative condition of $2a/L < 0.95$ for a given electron mobility μ , one obtains,

$$f_0 < \frac{0.431}{\sqrt{\mu}} \quad (18)$$

Fig. 4 Absorption spectra for the designed structure as a function of incidence angle and frequency for **a** TM polarization and **b** TE polarization

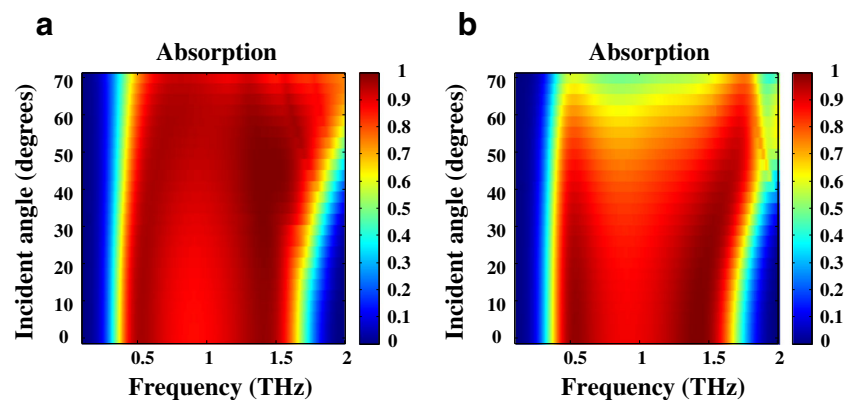
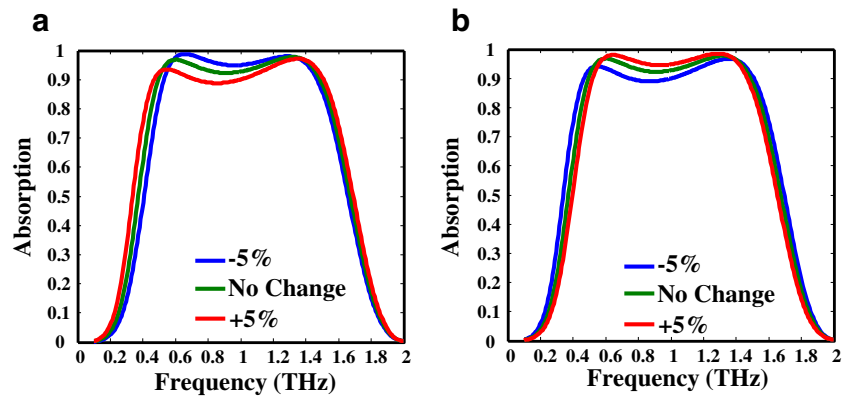


Fig. 5 Absorption spectra of the device affected by fractional variations of $\pm 5\%$ in the **a** disks radius and **b** arrays period



which is yielded from Eq. 15. We also know that the interest range of frequency for achieving a normalized bandwidth of 100 % is $0.5 f_0 < f_0 < 1.5 f_0$ leading to the minimum free-space wavelength $\lambda_{min} = n_s c / 1.5 f_0$. On the other hand, the proposed circuit model for the graphene disk arrays will be only valid for the array period smaller than the incident minimum wavelength. So, the second restriction is imposed by $L < \lambda_{min} = n_s c / 1.5 f_0$ resulting in the following lower limit on the central frequency using Eqs. 12–13 and 15–16:

$$f_0 > \frac{0.3}{\sqrt{\mu}} \tag{19}$$

For the numerical example of the previous section with the given electron mobility $\mu = 0.2 \text{ m}^2/Vs$, the absorber will be able to operate in the frequency range of $0.708\text{THz} < f_0 < 1.02\text{THz}$. However, it is possible

to move to a higher frequency by decreasing the electron mobility. Another method to design a broadband absorber at higher frequencies is to modify the Eq. 12 as follows:

$$\tau = \frac{n_s}{\beta f_0 8\alpha} \tag{20}$$

where β is smaller than unity and is considered reverse of the increased central frequency to keep βf_0 constant. Accordingly, the increased central frequency varies in the frequency range of $(0.5/\beta) f_0 < f_0 < (1.5/\beta) f_0$ which the upper limit obviously moves toward higher frequencies. By setting $\beta = 0.5$ and $f_0 = 2 \text{ THz}$, the parameters of the desired broadband absorber are as follows: $d = 25 \mu\text{m}$, $\tau = 1.07 \times 10^{-13} \text{ s}$, $E_f = 0.595 \text{ eV}$, $a = 12.4 \mu\text{m}$, and $L = 26.53 \mu\text{m}$. The corresponding absorption spectrum is plotted in Fig. 7 showing a normalized bandwidth of 85 %. As a result, higher central frequency (smaller β) leads to

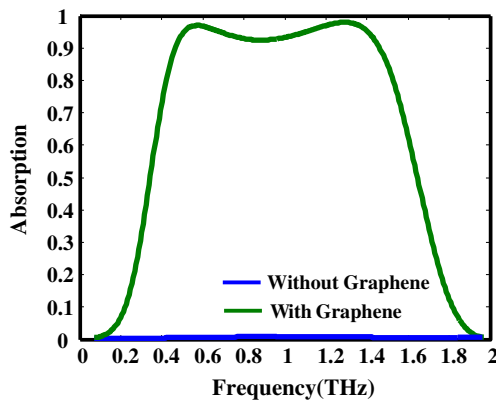


Fig. 6 The effect of the patterned graphene layer on absorption: As seen, the absorption of the device is attributed to the presence of graphene disks

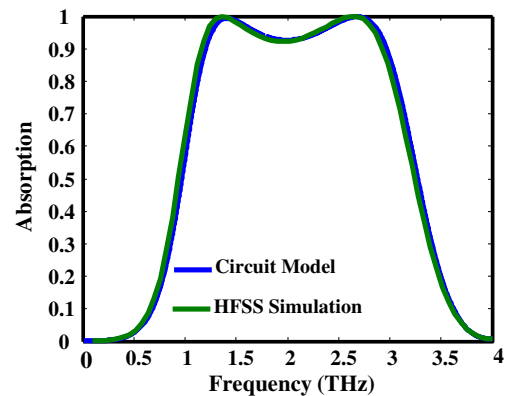


Fig. 7 Simulated absorption spectrum of the the designed device around the central frequency of $f_0 = 2 \text{ THz}$ with $\beta = 0.5$ using the proposed circuit model and the HFSS simulation

decrease of the bandwidth. Therefore, there is a trade off between the normalized bandwidth and the upper operating frequency.

Conclusion

In summary, a polarization-independent and ultra-broadband absorber was designed using impedance matching concept in the terahertz regime. First, we assigned an equivalent circuit to the absorber. We then adjusted the real part of the circuit input admittance to be close to the free space admittance. Imaginary part of the input admittance and its derivative were also set to zero at the central frequency. These properties for the input admittance of the device lead to almost impedance-matching condition in a wide range of frequencies. Thanks to the analytical circuit model, the parameters of the proposed structure were explicitly obtained for a given central frequency. It was demonstrated, through full-wave simulations, that the proposed absorber can maintain the absorption above 90 % over a wide range of frequencies (normalized bandwidth of 100 %).

We also examined the sensitivity of the device with respect to incident angle, polarization, and geometrical variations and a good robustness was observed.

It should be emphasized that the central frequency of the device cannot be chosen arbitrarily and it falls within a specific range which is roughly in the terahertz regime. This range is inversely proportional to the square root of the electron mobility of the graphene. However, the device can be designed at higher central frequencies at the cost of narrower bandwidth.

References

1. Ma W, Wen Y, Yu X (2013) Broadband metamaterial absorber at mid-infrared using multiplexed cross resonators. *Opt Express* 21:30724–30730
2. Panahi M, Abdollahramezani S, Ebrahimzadeh G, Safian R (2015) An efficient high power RF dummy-load. *IEEE Microwave Wireless Compon Lett* 25:409–411
3. Greffet J-J, Carminati R, Joulain K, Mulet J-P, Mainguy S, Chen Y (2002) Coherent emission of light by thermal sources. *Nature* 416:61–64
4. Pala RA, White J, Barnard E, Liu J, Brongersma ML (2009) Design of plasmonic thin-film solar cells with broadband absorption enhancements. *Adv Mater* 21:3504–3509
5. Cui Y, He Y, Jin Y, Ding F, Yang L, Ye Y, Zhong S, Lin Y, He S (2014) Plasmonic and metamaterial structures as electromagnetic absorbers. *Laser Photonics Rev* 8:495–520
6. Ye YQ, Jin Y, He S (2010) Omnidirectional, polarization-insensitive and broadband thin absorber in the terahertz regime. *JOSA B* 27:498–504
7. Grant J, Ma Y, Saha S, Khalid A, Cumming DR (2011) Polarization insensitive, broadband terahertz metamaterial absorber. *Opt Lett* 36:3476–3478
8. Duan X, Chen S, Liu W, Cheng H, Li Z, Tian J (2014) Polarization-insensitive and wide-angle broadband nearly perfect absorber by tunable planar metamaterials in the visible regime. *J Opt* 16:125107
9. Khavasi A (2015) Design of ultra-broadband graphene absorber using circuit theory. *JOSA B* 32:1941–1946
10. Barzegar-Parizi S, Rejaei B, Khavasi A (2015) Analytical circuit model for periodic arrays of graphene disks. *IEEE J Quantum Electron*:51
11. Abdollahramezani S, Arik K, Khavasi A, Kavehvash Z (2015) Analog computing using graphene-based metalines. *Opt Lett* 40:5239–5242
12. Abdollahramezani S, Arik K, Farajollahi S, Khavasi A, Kavehvash Z (2015) Beam manipulating by gate-tunable graphene-based metasurfaces. *Opt Lett* 40:5383–5386
13. Farajollahi S, Abdollahramezani S, Arik K, Khavasi A, Rejaei B (2015) Circuit model for plasmons on graphene with one dimensional conductivity profile. *Photon Technol Lett* 28:355–358